Int j simul model 23 (2024) 4, 622-633
Original scientific paper

PARAMETER OPTIMIZATION AND ANALYSIS OF PLASTIC SEPARATOR BASED ON EDEM-FLUENT

San, Y. L.[*,#]; Li, Y. M.[*]; Xiao, S. H.[*]; Zhang, C. Y.[*] & Liu, Y. B.[**]
[*] School of Mechanical Engineering, Hubei Engineering University, Xiaogan 432000, China
[**] Key Laboratory of Modern Agricultural Equipment and Technology, Ministry of Education, Jiangsu University, Zhenjiang 212013, China
E-Mail: sanyunlong@163.com ([#] Corresponding author)

Abstract
The rapid and efficient separation of polyethylene terephthalate (PET) materials from the crushed beverage bottle mixture is one of the current technical difficulties. In this study, a gas–solid phase flow model of broken beverage bottle materials was established, and a simulation analysis of winnowing separation process of the broken beverage bottle mixed material was performed utilizing the engineering data exchange model (EDEM) and the computational fluid dynamics (CFD). A four-factor and three-level response surface method (RSM) was designed to investigate the influences of material feed weight (*A*), wind velocity (*B*), wind velocity angle (*C*) and initial material feeding velocity (*D*) on the separation effect. The PET material content (C_{PET}) after separation was applied as evaluation index to determine the optimal winnowing parameters. Results show that the EDEM-Fluent coupling simulation can reflect the impact of fluid parameters on movement paths of the mixed material. The influencing strength of factors on separation rate was concluded as follows: $B > D > C > A$. The results obtained with optimized parameters showed that the C_{PET} approaches 99.99 % accuracy.
(Received in August 2024, accepted in November 2024. This paper was with the authors 1 month for 1 revision.)

Key Words: Plastic Recycling, PET, Winnowing Separation, EDEM-Fluent Coupling, Response Surface Method

1. INTRODUCTION

Polyethylene terephthalate $(C_{10}H_8O_4)_n$ or known as PET, is a type of light, low-cost polymer material with good mechanical performances. PET has been extensively applied to production and manufacturing of beverage bottles. At present, the recovery rate of beverage bottles in developing countries is only 94 %, which is considerably lower than those in developed countries in Europe and America [1, 2]. As shown in Fig. 1, common beverage bottles are composed of bottle body (PET material) and label paper (Biaxially oriented polypropylene film – BOPP material). PET material is specifically the major object for recycling and reuse. If the recycled PET purity is not satisfactory (< 99.95 %), then there may be some underlying concerns, such as silk and outlet breakages, during the secondary processing of recycled silk, thereby influencing the secondary processing and shaping effect of PET [3, 4]. Manual removal, chemical processing, and floating separation are traditional ways to separate beverage bottle body and labels. Manual separation is the major separation method at present (see Fig. 2), this method incurs high labour intensity and low efficiency. In addition, chemical treatment has high cost, poor safety, and causes environmental pollution and other problems. Furthermore, the floating separation method encounters difficulty in effectively separating PET and BOPP with similar density [5, 6]. For high-efficiency separation and screening of the broken bottle body and label mixture, the winnowing separation method based on fluid mechanics becomes a widely using method due to its simple structure and high efficiency [7, 8]. However, the winnowing process involves many factors, bringing immense challenges in studying the structural design of winnowing devices, construction of flow field model, and interactive influences of working parameters, among others.

Figure 1: Beverage bottle.

Figure 2: Manual separation of plastic bottles and trademarks.

Numerous studies on winnowing flow field analysis and selection of working parameters have been conducted [9]. However, the motion laws of solid particles in the flow field and interactive influences of parameters are still ambiguous. Given the increasing interactive influencing factors that have to be considered during the construction of fluid and solid models, among the key concerns that must be addressed immediately include how to improve the coupling analysis accuracy of two complicated models, determine practical influences of parameters on winnowing, and realize high-efficiency mechanical winnowing. Therefore, how to construct accurate a gas–solid phase coupling model and determine the major parameters influencing the winnowing process, resulting in high-efficiency and high-purity winnowing of PET materials, exhibit engineering significance.

Based on the simulation analysis and experiments, this study uses the EDEM-Fluent coupling simulation model to analysis the motion laws of materials in wind field, and the influence separation process key factors. Through RSM analysis and multi-factor combined test, winnowing parameters are optimizes systematically.

2. STATE OF THE ART

Based on the differences of materials in density, shape, and surface characteristics, winnowing of solid mixed material by using high-speed airflow is among the current major mechanical sorting techniques [10]. For the winnowing machine design, many scholars have studied the influences of wind velocity angle [11], vibrational frequency [12], suspension speed [13], and other factors on material separation. Wang et al. [14] changed the air velocity angle by changing the wind shield angle, thereby improving separation efficiency through coupling calculation. Teklemariyem et al. [15] studied and optimized the geometric parameters of air diffuser in wind turbine through the computational fluid dynamics (CFD) technology. Studies on winnowing simulation analysis include discrete element analysis (DEM) [16], multi-factor analysis [17], and mathematical model analysis [18]. Wang et al. [19] gained optimization parameters of peanut picker based on the DEM technology, but the hydromechanics was not verified. Cao et al. [20] analysed the influences of multiple parameters on movement paths of walnut winnowing, and a prototype was produced for a verification experiment. However, research applications were only applicable to winnowing of large-size materials. Li et al. [21] constructed a gas–solid phase coupling model through the CFD-DEM coupling method and gained combinations of the optimal working parameters through the single-factor simulation and multi-factor combined tests. However, the accuracy of the optimization results should be further improved.

Although the aforementioned studies have achieved relative progress in winnowing technology [22-24], there are limitations in coping with the complicated interaction of materials and multi-factor comprehensive influences. Moreover, building a simulation model for processing the complicated interaction of multi-phase flow physical fields is considerably difficult, and uncertainty of results increased [25-27]. Therefore, this study proposes a gas–

solid phase coupling simulation method and multi-factor combined test that can provide references for winnowing parameter optimization.

The remainder of this study is organized as follows. Section 3 measures basic parameters of PET and BOPP material, builds and designs the EDEM-Fluent coupling simulation model and RSM. Section 4 establishes and analyses the regression model according to RSM results, and optimized and verified the target function. Section 5 summarizes the conclusions drawn from this study.

3. METHODOLOGY

3.1 Characteristic analysis of plastic bottle mixed material

Beverage bottles are broken into lamellar PET/BOPP mixed materials (see Fig. 3). After breaking the same batch of beverage bottles, five mixed material samples (200 g/sample) were chosen randomly. The weight of single material piece in each sample was measured using an electronic balance with an accuracy of 0.001 g. In addition, the maximum length *a*, width *b*, and thickness *c* of single material piece were measured by using a vernier calliper with an accuracy of 0.01 mm. The mean results were used as basic dimensional sizes. The measurement method is shown in Fig. 4. Lastly, means of five mixed material samples were used as test results in this study. The measured results are: the average dimensions of a single PET piece are 19.79 × 15.20 × 0.3 mm, while the average dimensions of a single BOPP piece are 20.75 × 15.05 × 0.05 mm. Similarly, the average weight of a single PET piece is 0.15 g, while the average weight of a single BOPP piece is 0.01 g.

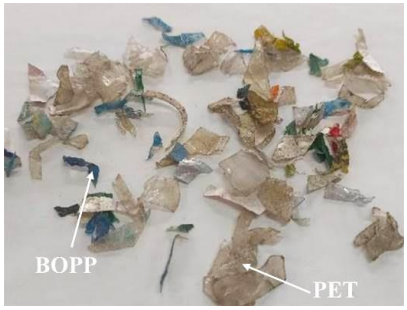

Figure 3: PET/BOPP mixed materials.

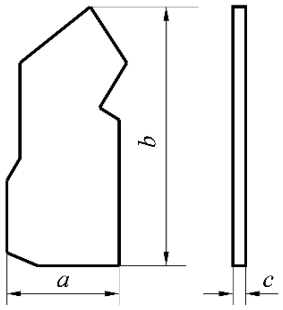

Figure 4: Measurement of the material's external dimensions.

The equivalent diameter of the mixed particle is solved as follows:

$$d_s = 1.24\left(\frac{m}{\rho_s}\right)^{\frac{1}{3}} \tag{1}$$

where d_s is the equivalent spherical diameter (m), m is the material mass (g), ρ_s is the material density (g/cm^3).

Densities of PET and BOPP used in standard production of beverage bottles at present are 1.37 g/cm^3 and 0.91 g/cm^3, respectively. Combining with the basic properties of materials, the equivalent diameter of PET bottles (d_{SP}) was calculated as 5.94 mm and the equivalent diameter of BOPP (d_{SB}) was 2.76 mm.

3.2 Winnowing device and analysis of mixed materials

Winnowing is to separate PET and BOPP materials through their settlement laws under the stress in air medium. Materials gain the initial forward moving velocity in the falling process through air flue, and then make drifting movement in the box of the draught fan. Different

material components were separated through differences in horizontal drifting distance owing to their different weights. In this study, the RLFX-1 mode PET winnowing machine produced by Hubei RUILI Environmental Protection Device Co., Ltd. (see Fig. 5) was analysed and tested.

Figure 5: RLFX-1 mode multi-level PET winnowing machine.

During the winnowing of broken plastics, the motion characteristics of mixed materials and relevant parameters of winnowing device may directly influence the winnowing results. By building a material drifting model, the movement of materials in the winnowing chamber under the influence of airflow was analysed by building a material drifting model. Moreover, the stresses on broken plastics were analysed. As shown in Fig. 6, plastic particles were viewed as the mass point under the action of airflow to build a coordinate system. The material inlet was used as the origin of the coordinate system. Meanwhile, the horizontal direction of winnowing chamber was used as the *x*-axis, and the direction perpendicular to the *x*-axis is the *y*-axis. Wind velocity at the air outlet is u and its included angle with the *x*-axis is α. The initial material velocity in airflow is v_0 and the initial included angle (β) between the materials and *y*-axis is 0°.

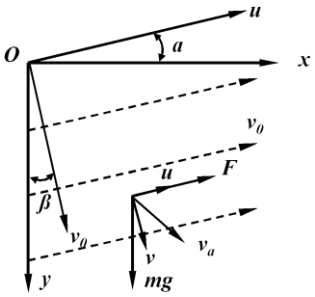

Figure 6: Force analysis of the mixed plastics.

The relative movement velocity v_r (m/s) of the mixed materials is as follows:

$$\overline{v_r} = \overline{v_a} + \overline{u} \tag{2}$$

where v_a is the absolute velocity of the materials (m/s) and u is the wind velocity (m/s).

The action force of airflow on materials is calculated as the driving force F_R (N) and is deduced as follows:

$$F_R = C\frac{\pi}{4}d_S^2\rho_a\frac{v_r^2}{2} \tag{3}$$

Where F_R is the driving force (N).

The PET/BOPP dynamic differential equation is as follows:

$$\begin{cases} F_R = m\dfrac{dv_{ax}}{dt} \\ W_S - F_R = m\dfrac{dv_{ay}}{dt} \end{cases} \tag{4}$$

where v_{ax} is the velocity in *x* direction (m/s), v_{ay} is the velocity in *y* direction, W_S is the resultant force in the *y* direction.

The initial velocity of materials is as follows:

$$\begin{cases} v_{ax_0} = v_0 \sin\alpha \\ v_{ay_0} = v_0 \cos\alpha \end{cases} \tag{5}$$

where v_0 is the initial velocity (m/s), v_{ax0} is the initial velocity in x direction (m/s), v_{ay0} is the initial velocity in y direction (m/s).

Suppose the time length (Δt) is the step length. Accordingly, v_{axn} and v_{ayn} are set as two-dimensional components of velocity at any moment. Moreover, $v^*_{ax_{n+1}}$ and $v^*_{ay_{n+1}}$ are approximate values of the two-dimensional components of Δt. The average instantaneous separation rate before and after Δt was chosen as the separation rate at calculation. On this basis, the result is as follows:

$$\begin{cases} v_{ax_{n+1}} = v_{ax_n} + \Delta t \times 0.5 \times \left[f_1\left(v_{axn},\ v_{ayn}\right) + f_1\left(v^*_{ax+1},\ v^*_{ay+1}\right) \right] \\ v_{ay_{n+1}} = v_{ay_n} + \Delta t \times 0.5 \times \left[f_2\left(v_{axn},\ v_{ayn}\right) + f_2\left(v^*_{ax+1},\ v^*_{ay+1}\right) \right] \end{cases} \tag{6}$$

The horizontal and vertical velocity values of the mixed material particles in a tiny period (Δt) can be viewed as the mean between material and terminal velocities, thereby obtaining the displacement of the mixed materials. X_n and Y_n are set as two-dimensional components of displacement at any moment.

$$\begin{cases} \Delta X_n = 0.5\left(v_{ax_{n+1}} + v_{axn}\right)\Delta t \\ \Delta Y_n = 0.5\left(v_{ay_{n+1}} + v_{ayn}\right)\Delta t \end{cases} \tag{7}$$

Therefore, the displacement of the mixed material particles can be deduced as follows:

$$\begin{cases} \Delta X_{n+1} = X_n + \Delta X_n \\ \Delta Y_{n+1} = Y_n + \Delta Y_n \end{cases} \tag{8}$$

3.3 Winnowing test of the PET/BOPP mixture

To obtain the combination of optimal winnowing parameters and to optimize parameters of the winnowing machine, relevant tests were conducted using EDEM and Fluent simulation software according to the built model and analysis results.

Movement of solid particles in the flow field was analysed based on gas–solid phase model theory. According to the basic properties of materials and relevant parameters of the RLFX-1 mode multi-level PET winnowing machine (see Table I), the EDEM and Fluent air box flow field models were built (see Fig. 7). The model consists of a feeding inlet, air inlet, five air outlets, and the corresponding particle collection box.

Table I: Material parameters.

Material	**Poisson's ratio**	**Shear modulus** (MPa)	**Density** ($kg \cdot m^{-3}$)
PET	0.37	1.2×10^3	1370
BOPP	0.4	1.5×10^3	910
Galvanized sheet	0.3	8×10^4	7850
Material-Material	**Recovery factors**	**Static friction coefficients**	**Dynamic friction coefficients**
PET-PET	0.44	0.27	0.1
BOPP-BOPP	0.25	0.3	0.1
PET-BOPP	0.25	0.5	0.01
PET-Galvanized sheet	0.2	0.5	0.01
BOPP-Galvanized sheet	0.32	0.5	0.01

The process of the EDEM-Fluent coupling simulation is shown in Fig. 8. Movements of two types of material particles in the winnowing chambers were simulated.

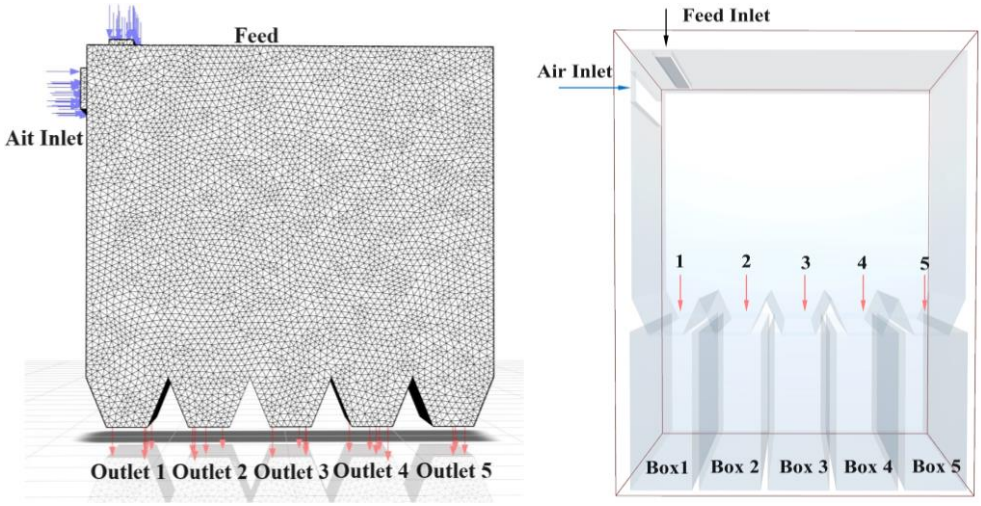

a) b)

Figure 7: Air box model: a) ANSYS model, b) EDEM model.

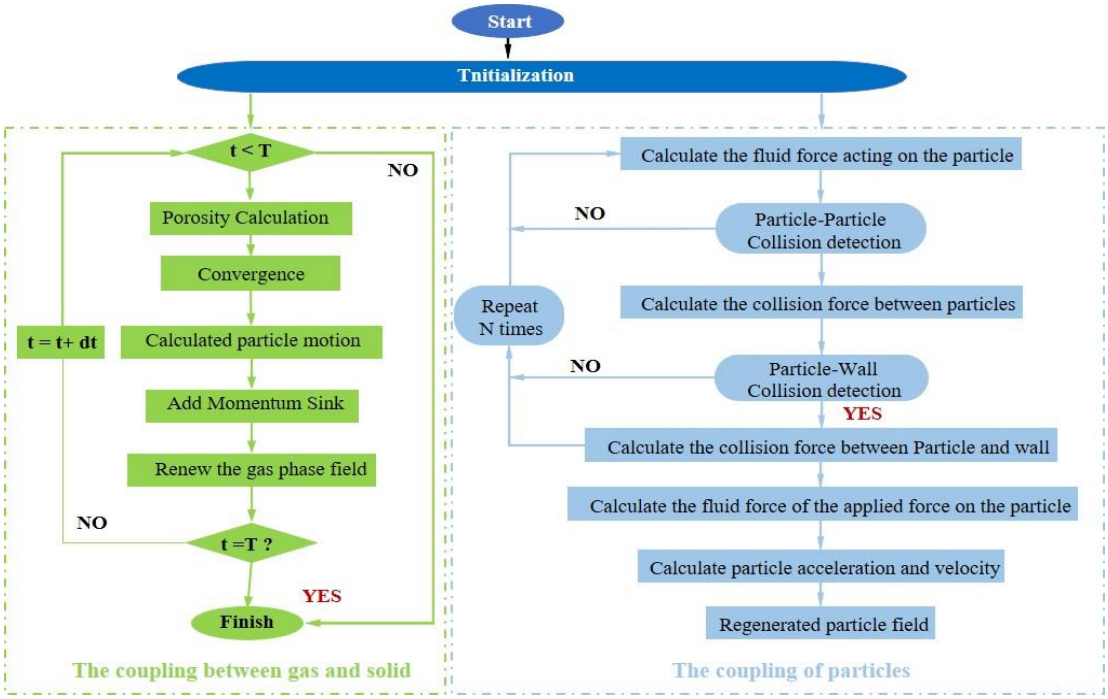

Figure 8: EDEM-Fluent coupling flow diagram.

The EDEM-Fluent coupling simulation test was conducted based on preceding parameters (see Figs. 9 and 10). When the included angle between material falling and vertical direction (β) is 0° (materials fall vertically), the movement paths of the materials in the two-dimensional plane spaces can be gained by combining with the stress analysis and kinematical equation of the PET/BOPP mixture (Fig. 11). Ranges of wind velocity angle α (0° to 50°), initial material feeding velocity v_0 (0 to 5 m/s), and wind velocity v_f (0 to 7 m/s) were adjusted. The relation curves between parameters and horizontal displacements are shown in Fig. 12.

According to movement paths and related curves of the mixed materials, the wind velocity angle, initial material feeding velocity, and wind velocity significantly influence the horizontal displacements of materials during vertical falling. Horizontal distance among different types of materials increases with an increase in parameters. Accordingly, choosing the relevant parameters in the reasonable ranges is conducive to separate PET and BOPP in the mixed materials.

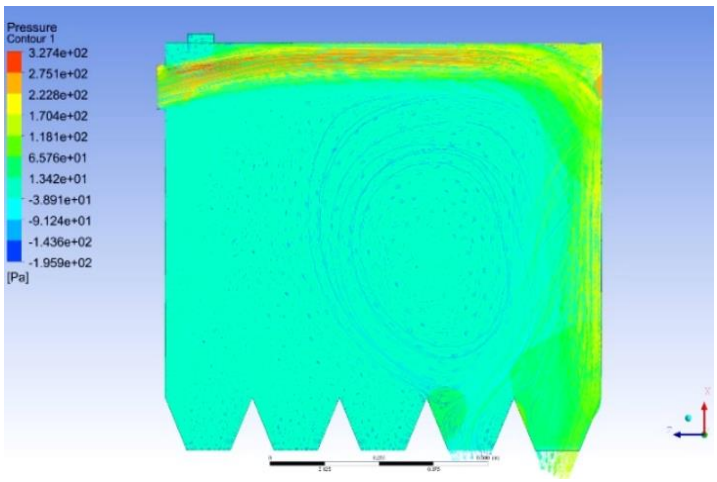

Figure 9: Pressure and velocity vector diagram.

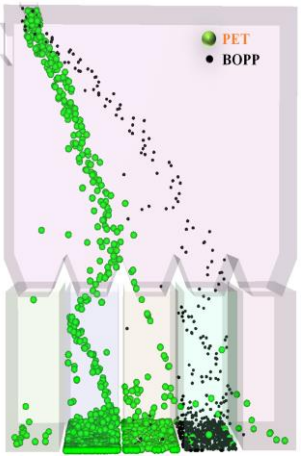

Figure 10: EDEM-Fluent coupling analysis process diagram.

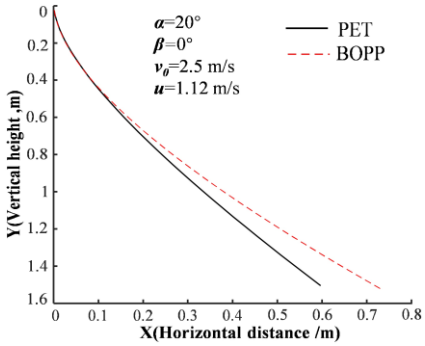

Figure 11: Movement path of the material in the *xoy* plane.

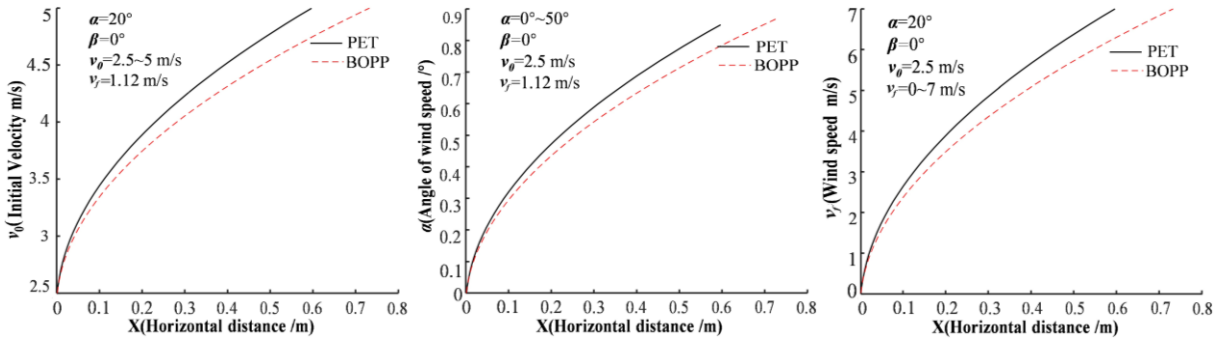

a) b) c)

Figure 12: The relation curves between parameters and horizontal displacements; a) Initial velocity and horizontal displacement, b) Wind velocity angle and horizontal displacement, c) Wind speed and horizontal displacement.

3.4 RSM design

According to the production efficiency of devices in practical production, the broken plastic bottles accumulate at air outlets when feed weight exceeds a certain value. Such a material accumulation may break the uniform distribution of materials and may also hinder effective airflow, thereby influencing material sorting. RSM, combined with simulation analysis results, was conducted by combining material feed weight *A* (g/s), winnowing air outlet velocity *B* (m/s), wind velocity angle *C* (°), and initial material feeding velocity *D* (m/s). The proportion of the PET particles (C_{PET}) in the mixed materials collection boxes 1 and 2 at the outlet was chosen as the evaluation index:

$$C_{PET} = \frac{\text{Particle number of PET}}{\text{Particle number of PET+Particle number of BOPP}} \times 100\% \quad (9)$$

A four-factor three-level RSM was built. The test factors and levels are shown in Table II. The test design scheme and response results are shown in Table III.

Table II: Test factors and levels.

Level	**Factor**			
	A (g/s)	***B*** (m/s)	***C*** (°)	***D*** (m/s)
-1	36	15	0	0
0	56	20	15	1
1	76	25	30	2

Table III: The test design scheme and response results.

Test number	***A*** (g/s)	***B*** (m/s)	***C*** (°)	***D*** (m/s)	C_{PET} (%)
1	0	0	-1	-1	99.06
2	0	-1	0	1	67.90
3	0	-1	0	-1	69.43
4	0	1	1	0	76.30
5	0	0	-1	0	87.99
6	0	0	1	-1	99.43
7	0	0	0	0	95.31
8	1	-1	0	0	67.88
9	0	1	0	1	75.52
10	0	0	-1	1	67.58
11	0	0	1	1	67.58
12	0	0	0	0	95.83
13	-1	1	0	0	99.96
14	0	-1	-1	0	67.60
15	0	1	-1	0	73.75
16	0	0	0	0	95.62
17	1	0	-1	0	82.46
18	0	-1	1	0	67.56
19	-1	-1	0	0	67.56
20	1	0	0	1	74.56
21	1	1	0	0	99.69
22	0	1	0	-1	99.58
23	-1	0	0	-1	99.04
24	-1	0	0	-1	99.69
25	-1	0	1	0	79.67
26	0	0	0	0	95.19
27	-1	0	-1	0	84.41
28	1	0	1	0	88.78
29	-1	0	0	1	67.58

4. RESULT ANALYSIS AND DISCUSSION

4.1 Test result analysis and construction of the regression model

According to the regression analysis of the test results and multi-element fitting analysis, the regression equation of C_{PET} at the outlet and its significance were gained. The significance analysis results of the test are shown in Table IV.

According to the analysis, the overall model linearity is extremely significant ($P < 0.01$), and the fitting regression equation is as follows:

$$C_{\mathrm{PET}} = -1.5164 + 0.2118v_f + 0.1429v_0 - 0.0045v_f^2 - 0.0004\alpha^2 \tag{10}$$

The coefficient of determination (R^2) of the model is 0.8631, and the fitting degree is high. According to Table IV, the rest of the items can influence the separation rate significantly except for *A*, *C*, *AB*, *AC*, *AD*, *BC*, *BD*, *CD*, A^2, and D^2. Without consideration to interactive influences, the influencing strength of factors on separation rate has the following order: $B > D > C > A$. That is, Wind velocity v_f > Initial material feeding velocity v_0 > Wind velocity angle α > Material feed weight *m*.

Table IV: Regression model variance test and analysis.

Source of variation	**Sum of squares**	***df* freedom**	***F***	***P*-value Prob > *F* square**	
Model	0.43	14	6.30	0.0007	significant
A	$1.528 \cdot 10^{-3}$	1	0.32	0.5822	
B	0.11	1	23.63	0.0003	
C	$1.658 \cdot 10^{-4}$	1	0.0034	0.8555	
D	0.18	1	36.64	<0.0001	
AB	$8.703 \cdot 10^{-6}$	1	$1.807 \cdot 10^{-3}$	0.9667	
AC	$3.058 \cdot 10^{-3}$	1	0.63	0.4388	
AD	$1.455 \cdot 10^{-3}$	1	0.30	0.5912	
BC	$1.677 \cdot 10^{-4}$	1	0.035	0.8546	
BD	0.013	1	2.63	0.1268	
CD	$3.422 \cdot 10^{-6}$	1	$7.106 \cdot 10^{-4}$	0.9791	
A^2	$1.507 \cdot 10^{-3}$	1	0.31	0.5847	
B^2	0.083	1	17.33	0.0010	
C^2	0.049	1	10.11	0.0067	
D^2	0.014	1	2.81	0.1160	
Residual	0.067	14			
Lack of Fit	0.063	10	5.56	0.0563	not significant
Pure Error	$4.522 \cdot 10^{-3}$	4			
Cor Total	0.49	28			

Note: $P < 0.01$, extremely significant; $0.01 < P < 0.05$, significant; $P > 0.05$, not significant; * is none.

To further investigate the influences of factors on C_{PET}, the response surfaces and contour maps influenced by the test index were gained after data processing (see Fig. 13). As shown in Fig. 13, C_{PET} increases initially and decreases thereafter with an increase in feed weight and wind velocity, an increase in wind velocity and wind velocity angle, an increase in wind velocity and initial speed, or an increase in wind velocity angle and initial speed. Moreover, it presents an increasing trend with an increase in feed weight and wind velocity angle. However, it shows no evident changes with an increase in feed weight and initial speed.

4.2 Optimal solving of parameters and verification

According to the basic principle of winnowing, a multi-target optimization analysis of the preceding test data was to assure that PET purity after separation meets the recycling and reuse requirements. The target coding variable optimization function is as follows:

$$\max C_{PET}(A,B,C,D), \begin{cases} 36 \leqslant A \leqslant 76 \\ 15 \leqslant B \leqslant 25 \\ 0 \leqslant C \leqslant 30 \\ 0 \leqslant D \leqslant 2 \end{cases} \tag{11}$$

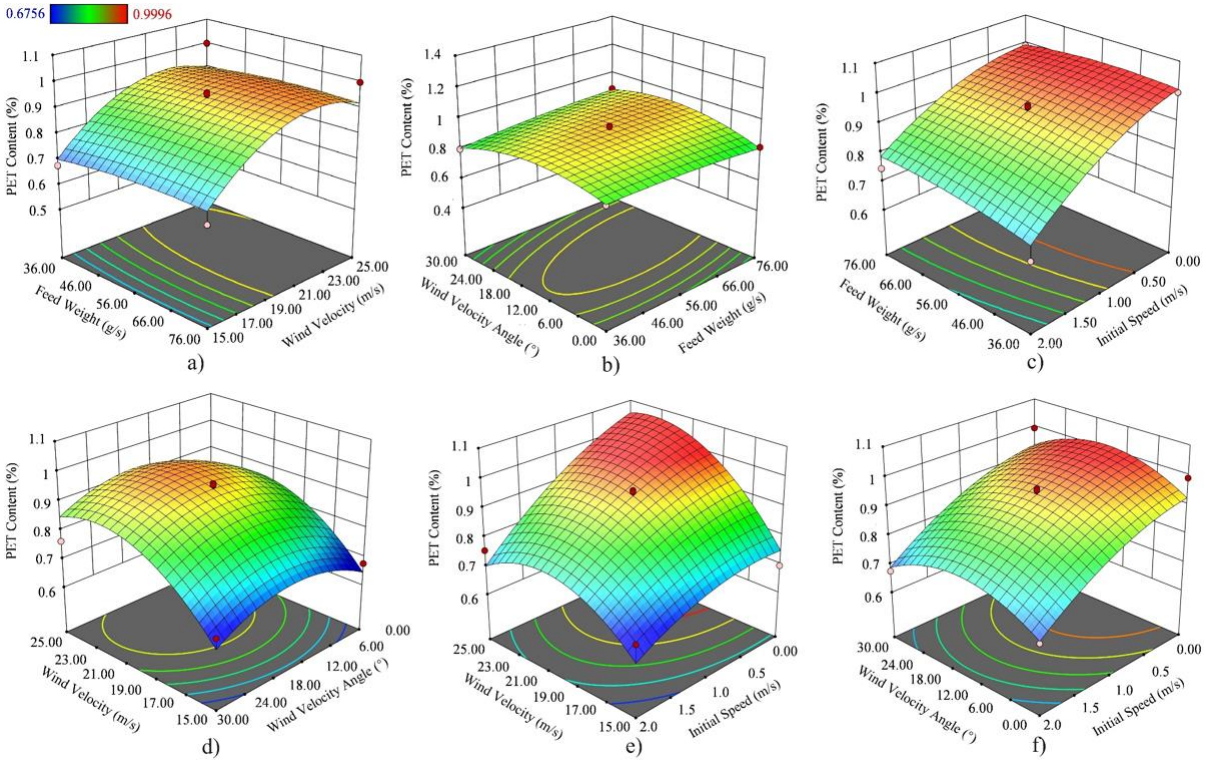

Figure 13: Influences of various factors on separation rate: a) Feed weight and Winnowing air outlet velocity, b) Feed weight and wind velocity angle, c) Feed weight and Initial material feeding velocity, d) Winnowing air outlet velocity and Wind velocity angle, e) Winnowing air outlet velocity and Initial material feeding velocity, f) Wind velocity angle and Initial material feeding velocity.

The target function was optimized to obtain the optimal winnowing parameters: feed weight of mixed materials is 59.08 g/s; wind velocity is 21.71 m/s; wind velocity angle is 18.01°; and initial falling velocity of materials is 0.18 m/s. According to optimization verification test results, the CPET value is 99.84 %. After transformation into mass, the proportion of PET in the total mass of mixed materials is 99.989251 %, which was rounded off to two decimal places. PET purity is 99.99 % (< 0.05 %), conforming the recycling and reuse requirements.

5. CONCLUSION AND FUTURE WORK

In this study, numerous EDEM-Fluent coupling simulations were performed to analyse the movement laws in the separation chambers of the beverage bottle mixed materials. The influences of winnowing parameters on material winnowing effect were investigated. The following conclusions were drawn from this study:

(1) When materials fall vertically, the wind velocity angle, initial material feeding velocity, and wind velocity can significantly influence the horizontal displacement of different materials. Horizontal distance among the different types of materials may increase with an increase in parameters.

(2) Without considering interactive influences, wind velocity is the primary influencing factor of the winnowing separation rate, followed by the initial material feeding velocity, wind velocity angle, and material feed weight. The coefficient of determination of the regression equation is 0.8631.

(3) According to the optimal parameters gained from the target coding variable optimization function, PET purity is verified to be 99.99 %, conforming the recycling and reuse requirements of the PET materials.

The built model has some differences owing to the different basic parameters of different plastic materials. The coupling model will be further corrected in future studies to obtain considerably accurate simulation results.

ACKNOWLEDGEMENT

The study was supported by Scientific Research Guidance project of the Education Department of Hubei Province (No. B2022179) and Natural Science Foundation Project of Hubei Province (No. 2022CFB533).

REFERENCES

[1] Pál, V. (2024). Trouble with the bottle beverage containers and the widening waste crisis in socialist Hungary, *Journal of Contemporary History*, Vol. 59, No. 2, 293-312, doi:10.1177/00220094231225385

[2] Oda, K.; Wlodawer, A. (2024). Development of enzyme-based approaches for recycling PET on an industrial scale, *Biochemistry*, Vol. 63, No. 4, 369-401, doi:10.1021/acs.biochem.3c00554

[3] Fuentes, C. A.; Gallegos, M. V.; García, J. R.; Sambeth, J.; Peluso, M. A. (2020). Catalytic glycolysis of poly(ethylene terephthalate) using zinc and cobalt oxides recycled from spent batteries, *Waste and Biomass Valorization*, Vol. 11, No. 9, 4991-5001, doi:10.1007/s12649-019-00807-6

[4] Shi, J. X.; Zeng, W. W.; Li, J.; Xiang, Q. M.; Zhang, Y. L.; Zhang, D. H. (2013). The development of industrial yarn based on direct spinning technology with waste PET fiber, *Guangdong Chemical Industry*, Vol. 40, No. 23, 68-69

[5] Derr, K. M.; Lopez, C. V.; Maladeniya, C. P.; Tennyson, A. G.; Smith, R. C. (2023). Transesterification-vulcanization route to durable composites from post-consumer poly(ethylene terephthalate), terpenoids, and industrial waste sulfur, *Journal of Polymer Science*, Vol. 61, No. 23, 3075-3086, doi:10.1002/pol.20230503

[6] Mpika, S. A.; Nikolaidis, N. F.; Bikiaris, D. N.; Vouvoudi, E. C.; Lazaridis, N. K. (2023). Study on PET recovery from polymeric mixtures, using the floatation technique, and valorization of the collected particles by dyeing them, *Fibers and Polymers*, Vol. 24, No. 6, 1995-2008, doi:10.1007/s12221-023-00173-0

[7] Gall, M.; Wiener, M.; de Oliveira, C. C.; Lang, R. W.; Hansen, E. G. (2020). Building a circular plastics economy with informal waste pickers: recyclate quality, business model, and societal impacts, *Resources, Conservation and Recycling*, Vol. 156, Paper 104685, 11 pages, doi:10.1016/j.resconrec.2020.104685

[8] Blasenbauer, D.; Lipp, M.-A.; Fellner, J.; Tischberger-Aldrian, A.; Stipanović, H.; Lederer, J. (2024). Recovery of plastic packaging from mixed municipal solid waste: a case study from Austria, *Waste Management*, Vol. 180, 9-22, doi:10.1016/j.wasman.2024.02.040

[9] Tanguay-Rioux, F.; Spreutels, L.; Heroux, M.; Legros, R. (2022). Mixed modeling approach for mechanical sorting processes based on physical properties of municipal solid waste, *Waste Management*, Vol. 144, 533-542, doi:10.1016/j.wasman.2022.04.025

[10] Sahoo, R.; Swain, S. K.; Mahapatra, J.; Mohanty, D. K.; Mohapatra, P. M.; Dash, A. K. (2024). A study on moisture dependent properties of barnyard millet (Echinochloa frumentacea) grains, *Journal of Experimental Agriculture International*, Vol. 46, No. 6, 69-79, doi:10.9734/jeai/2024/v46i62458

[11] Ihnatiev, O.; Shevelova, H.; Strelnykov, H.; Blyuss, B. (2022). Numerical investigation of additional gas supply angle influence on flow in jet mill ejector, *IOP Conference Series: Earth and Environmental Science*, Vol. 970, Paper 012018, 8 pages, doi:10.1088/1755-1315/970/1/012018

[12] Zhang, F.; Li, L.; Ma, X. (2022). Simulation study on separation effect of mineral particles based on EDEM-FLUENT coupling, *Multipurpose Utilization of Mineral Resources*, Vol. 6, 159-166

[13] Aida, M.; Murakami, Y.; Shono, A. (2023). Estimation of the just suspension speed of mixed particles in a solid-liquid stirred tank, *Journal of Chemical Engineering of Japan*, Vol. 56, No. 1, Paper 2197949, 7 pages, doi:10.1080/00219592.2023.2197949

[14] Wang, H.; Fan, Y.; Liu, X.; Cai, P.; Tang, J.; Wu, J. (2021). Optimization of flotation chamber structure design based on EDEM-Fluent coupling, *Agricultural Equipment & Vehicle Engineering*, Vol. 59, No. 8, 76-80
[15] Teklemariyem, D. A.; Yimer, E. T.; Ancha, V. R.; Zeru, B. A. (2024). Parametric study of an empty diffuser geometric parameters and shape for a wind turbine using CFD analysis, *Heliyon*, Vol. 10, No. 5, Paper e26782, 25 pages, doi:10.1016/j.heliyon.2024.e26782
[16] Çalışkan, U.; Mišković, S. (2024). Analysis of particle dispersion and cavity formation during bulk particle water entry using fully coupled CFD-DEM-VOF approach, *Particuology*, Vol. 90, 558-580, doi:10.1016/j.partic.2023.12.018
[17] Rhee, S. M.; Kim, D. H.; Kim, M. S. (2024). Magnetic resonance imaging for relationship between the severity of perianchor fluid collection and rotator cuff integrity after arthroscopic double-row suture-bridge rotator cuff repair, *Orthopaedics & Traumatology: Surgery & Research*, Vol. 110, No. 5, Paper 103897, 6 pages, doi:10.1016/j.otsr.2024.103897
[18] Barakat, A.; Sun, B. (2024). Controlling TPMS lattice deformation for enhanced convective heat transfer: a comparative study of diamond and gyroid structures, *International Communications in Heat and Mass Transfer*, Vol. 154, Paper 107443, 14 pages, doi:10.1016/j.icheatmasstransfer.2024.107443
[19] Wang, B. K.; Yu, Z. Y.; Hu, Z. C.; Cao, M. Z.; Zhang, P.; Wang, B. (2021). Numerical simulation and experiment of flow field in three air systems of air separation system of peanut pickup harvester, *Journal of Agricultural Machinery*, Vol. 52, No. 11, 103-114, doi:10.6041/j.issn.1000-1298.2021.11.011
[20] Cao, C.; Luo, K.; Peng, M.; Wu, Z.; Liu, G.; Li, Z. (2019). Experiment on winnowing mechanism and winnowing performance of hickory material, *Chinese Society of Agricultural Machinery*, Vol. 50, No. 9, 105-112, doi:10.6041/j.issn.1000-1298.2019.09.012
[21] Li, H.; Zhang, M.; Yin, Y.; Zhang, H. (2023). Application of fluid-solid coupling method in agricultural engineering, *Journal of Chinese Agricultural Mechanization*, Vol. 44, No. 2, 20-28, doi:10.13733/j.jcam.issn.2095-5553.2023.02.004
[22] Bondarenko, O.; Boshkova, I. (2023). Evaluation of the efficiency of microwave heating of soils, *Technology Audit and Production Reserves*, Vol. 4, No. 1, 40-47, doi:10.15587/2706-5448.2023.286551
[23] Ramírez, J. M.; Castañon, F.; Espeche, J. (2023). A computational method for modeling the multi-physical interactions of electromagnetic wind energy harvesters in tandem arrangement, *Extreme Mechanics Letters*, Vol. 61, Paper 102028, 11 pages, doi:10.1016/j.eml.2023.102028
[24] Samaei, A.; Sang, Z. S.; Glerum, J. A.; Mogonye, J.-E.; Wagner, G. J. (2023). Multiphysics modeling of mixing and material transport in additive manufacturing with multicomponent powder beds, *Additive Manufacturing*, Vol. 67, Paper 103481, 18 pages, doi:10.1016/j.addma.2023.103481
[25] Al-Zawahreh, K.; Al-Degs, Y.; Barral, M. T.; Paradelo, R. (2022). Optimization of direct blue 71 sorption by organic rich-compost following multilevel multifactor experimental design, *Arabian Journal of Chemistry*, Vol. 15, No. 1, Paper 103468, 13 pages, doi:10.1016/j.arabjc.2021.103468
[26] Al-Baghdadi, M. A. R. S.; Al-Waily, M. (2021). Three-dimensional fluid-thermal-structure multiphysics interaction simulation model of aluminium extrusion process, *Journal of Mechanical Engineering and Sciences*, Vol. 15, No. 3, 8253-8261, doi:10.15282/jmes.15.3.2021.04.0648
[27] Rizzo, F.; Zazzini, P.; Montelpare, S.; Riccicutelli, A. (2020). Investigation of wind induced vibration and acoustic performance interactions for a flexible roof through multiphysics approach, *Journal of Building Performance Simulation*, Vol. 13, No. 5, 555-582, doi:10.1080/19401493.2020.1809015